Title	Superradiant terahertz emission by dipolaritons
Author(s)	Kyriienko, O.; Kavokin, A. V.; Shelykh, I. A.
Citation	Kyriienko, O., Kavokin, A. V., & Shelykh, I. A. (2013). Superradiant terahertz emission by dipolaritons. Physical review letters, 111(17).
Date	2013
URL	http://hdl.handle.net/10220/18645
Rights	© 2013 American Physical Society. This paper was published in Physical Review Letters and is made available as an electronic reprint (preprint) with permission of American Physical Society. The paper can be found at the following official DOI: [http://dx.doi.org/10.1103/PhysRevLett.111.176401]. One print or electronic copy may be made for personal use only. Systematic or multiple reproduction, distribution to multiple locations via electronic or other means, duplication of any material in this paper for a fee or for commercial purposes, or modification of the content of the paper is prohibited and is subject to penalties under law.

Superradiant Terahertz Emission by Dipolaritons

O. Kyriienko,[1,2] A. V. Kavokin,[3,4] and I. A. Shelykh[1,2]

[1]*Science Institute, University of Iceland, Dunhagi-3, IS-107 Reykjavik, Iceland*
[2]*Division of Physics and Applied Physics, Nanyang Technological University, 637371 Singapore*
[3]*School of Physics and Astronomy, University of Southampton, Highfield, Southampton SO17 1BJ, United Kingdom*
[4]*Spin Optics Laboratory, St. Petersburg State University, Building 1, Ulianovskaya Street, St. Petersburg 198504, Russia*
(Received 4 November 2012; revised manuscript received 17 June 2013; published 22 October 2013)

Dipolaritons are mixed light-matter quasiparticles formed in double quantum wells embedded in microcavities. Because of resonant coupling between direct and indirect excitons via electronic tunneling, dipolaritons possess large dipole moments. Resonant excitation of the cavity mode by a short pulse of light induces oscillations of the indirect exciton density with a characteristic frequency of Rabi flopping. This results in oscillations of a classical Hertz dipole array which generate supperradiant emission on a terahertz (THz) frequency. The resulting THz signal may be enhanced using the supplementary THz cavity in the weak coupling regime.

DOI: 10.1103/PhysRevLett.111.176401 PACS numbers: 71.36.+c, 07.57.Hm, 71.35.−y, 85.30.Mn

Introduction.—The generation and frequency modulation of terahertz radiation are among the major technological challenges nowadays [1]. Applications of terahertz sources span from communication technologies to medicine and security. The existing terahertz (THz) emitters are based on a large variety of physical principles [2]. One possible solution is a conventional solid state oscillator based on a high frequency Gunn or tunneling diode [3]. The operating frequency of such an oscillator is limited to the microwave region and the lower boundary of the terahertz range. Second, quantum cascade lasers (QCL) allow for coherent emission of radiation in a terahertz range [4,5]. Exploiting the multiple photon emission from intersubband transitions of wide quantum wells [6], QCL cover the upper boundary of THz range with a relatively high power of emission (up to 50 mW). QCL operate at cryogenic temperatures which strongly limits their application area. The laser driven terahertz emitters form a third group of THz sources, where a femtosecond optical pulse illuminating the semiconductor structure leads to an oscillation of carrier density which generates terahertz radiation [7–10]. Finally, the wide group of THz emitters are free electron based sources like klystron or a free electron laser. These are powerful but quite bulky sources. Optimization of spectral characteristics, size, efficiency, cost, and operation temperature of terahertz devices is one of the priority objectives of modern optoelectronics. Here, we propose a compact optical to terahertz radiation converter allowing for efficient frequency modulation and operation at high temperatures.

Theoretical proposals for THz sources in solid state and semiconductor physics present a rich diversity. One example is the use of carbon nanostructures, in particular, carbon nanotubes (CNTs) [11,12], or Aharonov-Bohm quantum rings [13]. Another area where a possibility of THz generation has been widely studied theoretically is *polaritonics*—the interdisciplinary research area at the boundary of solid state physics and quantum optics [14,15]. Polaritonic devices are based on the strong coupling between excitons in semiconductor quantum wells and confined photons. Proposals include the polariton based THz emitters where signal is generated from transitions between upper and lower polariton branches [16–18] and transition between $2p$ and $1s$ exciton states, the latter one strongly coupled to the cavity mode [19]. Recent theoretical studies also include the proposal for bosonic cascade lasers realized due to the multiple THz photon emission by excitons (exciton-polaritons) confined in a parabolic potential trap [20]. Our present proposal is based on the recent experimental realization of dipolaritons —cavity exciton-polaritons characterized by large dipole moments [21].

The mechanism for terahertz signal generation described in this Letter relies on the beats between spatially direct and indirect excitons. Spatially indirect excitons are composed of electrons and holes situated in separate quantum wells (QWs) [22]. Coupled QW systems, where the separation of electrons and holes and energy splitting between direct and indirect excitons can be controlled by applied electric fields, have been studied in the recent decades [23–25]. The radiative lifetimes of indirect excitons are usually much longer than those of direct excitons due to the lower electron–hole overlap. Another important feature of indirect excitons is their large dipole moments in the normal to QW plane direction, resulting in strong exciton-exciton interactions [26].

Recently, it has been shown that exciton polaritons and spatially indirect excitons can be intermixed in the biased semiconductor microcavities with embedded coupled QWs [21,27,28]. In these structures, new quasiparticles, which are a linear superposition of the cavity photon (C), direct exciton (DX), and indirect exciton (IX), appear. They form

three exciton-polariton modes, namely, the upper polariton (UP), middle polariton (MP), and lower polariton (LP) modes. These modes may be characterized by large dipole moments which is why they are referred to as *dipolaritons* [21]. Here, we study theoretically the effect of beats between dipolariton modes due to the tunnel coupling between direct and indirect excitons, which result into superradiant THz emission by an array of Hertz dipoles. Its characteristics can be tuned by the applied bias, and the calculated efficiency of proposed emitter is comparable with state-of-art generators.

The model.—The structure we consider represents two QWs separated by a barrier which is sufficiently thin to allow for resonant electron tunneling (Fig. 1). The electron wave function is shared between two QWs in this case. The optical microcavity is tuned to the wider QW exciton resonance (LQW in Fig. 1), while the right QW remains decoupled from the optical pump. Pulsed pumping creates electron-hole pairs which form direct excitons. The bias applied in the growth direction induces mixing of direct and indirect exciton states. Coupling of the cavity photons to direct excitons resulting in appearance of two polariton modes has been extensively studied [14,15]. The coupling and anticrossing of DX-IX resonances tuned by an electric field is also a well-known effect in GaAs/AlGaAs QW structures [29–31]. Both effects combined result in the appearance of dipolaritons studied recently by Cristofolini *et al.* [21].

The correct treatment of a real dipolariton system involves both coherent and decoherent parts for the Hamiltonian, $\hat{\mathcal{H}} = \hat{\mathcal{H}}_{\rm coh} + \hat{\mathcal{H}}_{\rm dec}$. The Hamiltonian corresponding to the coherent part reads

$$\hat{\mathcal{H}}_{\rm coh} = \hbar\omega_C \hat{a}^\dagger \hat{a} + \hbar\omega_{\rm DX} \hat{b}^\dagger \hat{b} + \hbar\omega_{\rm IX} \hat{c}^\dagger \hat{c} + \frac{\hbar\Omega}{2}(\hat{a}^\dagger \hat{b} + \hat{b}^\dagger \hat{a}) - \frac{\hbar J}{2}(\hat{b}^\dagger \hat{c} + \hat{c}^\dagger \hat{b}) + P\hat{a}^\dagger + P^* \hat{a}, \quad (1)$$

where $\hat{a}^\dagger$, $\hat{a}$, $\hat{b}^\dagger$, $\hat{b}$ and $\hat{c}^\dagger$, and $\hat{c}$ are creation and annihilation operators for cavity photons, direct excitons, and indirect excitons, respectively. Here, $\hbar\omega_C$, $\hbar\omega_{\rm DX}$, and $\hbar\omega_{\rm IX}$ denote cavity mode, direct exciton, and indirect exciton energies, and the first three terms of the Hamiltonian describe the energy of the bare modes. The fourth and fifth terms describe coupling between the modes, where Ω denotes the coupling constant between the photon and direct exciton, and the tunneling rate corresponding to DX-IX coupling is J. The last two terms in the Hamiltonian describe the optical pumping of cavity mode with amplitude $P(t) = P_0(t)e^{-i\omega_P t}$, where ω_P is a pumping frequency.

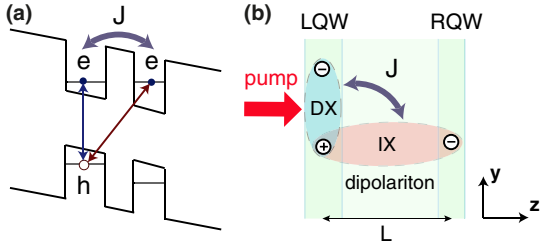

FIG. 1 (color online). Sketch of the system. (a) Double quantum well (DQW) heterostructure with resonantly coupled electron levels and a hole in the left quantum well (QW). The right QW has a larger bandgap than the left QW tuned by the presence of an indium alloy or the width of the well. (b) Electron-hole bilayer with schematic picture of coupled spatially indirect and direct exciton which form a dipolariton.

The decoherent part of dynamics of the system is mainly governed by the radiative lifetimes of the modes and phonon-scattering processes, which lead to population of thermalized exciton reservoirs [32]. They can be described by the exciton-phonon interaction Hamiltonian $\hat{\mathcal{H}}_{\rm int} = \hat{\mathcal{H}}^+ + \hat{\mathcal{H}}^-$, where

$$\hat{\mathcal{H}}^+ = D_{\rm DX}\sum_k \hat{b}^\dagger \hat{b}_{R,k}\hat{d}_k^\dagger + D_{\rm IX}\sum_k \hat{c}^\dagger \hat{c}_{R,k}\hat{d}_k^\dagger, \quad (2)$$

$$\hat{\mathcal{H}}^- = D_{\rm DX}\sum_k \hat{b}_{R,k}^\dagger \hat{b}\hat{d}_k + D_{\rm IX}\sum_k \hat{c}_{R,k}^\dagger \hat{c}\hat{d}_k, \quad (3)$$

correspond to processes with emission ($\hat{d}_k^\dagger$) and absorption ($\hat{d}_k$) of phonon with in-plane momentum k, respectively. Here, $\hat{b}_{R,k}^\dagger$, $\hat{b}_{R,k}$, $\hat{c}_{R,k}^\dagger$, and $\hat{c}_{R,k}$ are creation and annihilation operators for direct and indirect excitons in reservoirs. $D_{\rm DX,IX}$ denote exciton-photon interaction constants. These incoherent processes can be conveniently treated using master equation for the density matrix, $i\hbar\partial\rho/\partial t = [\hat{\mathcal{H}}_{\rm coh}, \rho] + \hat{\mathcal{L}}\rho^{(\rm dis)} + \hat{\mathcal{L}}\rho^{(\rm th)}$, where $\hat{\mathcal{L}}\rho^{(\rm dis)}$ corresponds to standard Lindblad superoperator describing the finite lifetime of the modes [17,19], and $\hat{\mathcal{L}}\rho^{(\rm th)}$ is responsible for phonon-assisted processes (see details of derivation in the Supplemental Material [32]).

In the following, we shall be interested in the large occupation numbers of the modes, and the mean-field approximation can be applied. The dynamics of the occupation numbers of the modes can be found from the master equation with operators treated as classical fields [32]

$$\partial\langle\hat{a}\rangle/\partial t = -i\Omega\langle\hat{b}\rangle/2 - \gamma_C\langle\hat{a}\rangle/2 - i\tilde{P}, \quad (4)$$

$$\partial\langle\hat{b}\rangle/\partial t = i\delta_\Omega\langle\hat{b}\rangle - iJ\langle\hat{c}\rangle/2 - i\Omega\langle\hat{a}\rangle/2 - \gamma_{\rm DX}\langle\hat{b}\rangle/2 + W\sum_k(\langle\hat{b}_{R,k}^\dagger\hat{b}_{R,k}\rangle - n_{{\rm ph},k})\langle\hat{b}\rangle, \quad (5)$$

$$\partial\langle\hat{c}\rangle/\partial t = i(\delta_\Omega - \delta_J)\langle\hat{c}\rangle - iJ\langle\hat{b}\rangle/2 - \gamma_{\rm IX}\langle\hat{c}\rangle/2 + W\sum_k(\langle\hat{c}_{R,k}^\dagger\hat{c}_{R,k}\rangle - n_{{\rm ph},k})\langle\hat{c}\rangle, \quad (6)$$

$$\partial\langle\hat{b}^{\dagger}_{R,q}\hat{b}_{R,q}\rangle/\partial t = -\gamma_{\mathrm{DX}}\langle\hat{b}^{\dagger}_{R,q}\hat{b}_{R,q}\rangle + W\sum_{k}\{|\langle\hat{b}\rangle|^2(\langle\hat{b}^{\dagger}_{R,k}\hat{b}_{R,k}\rangle + 1)n_{\mathrm{ph},k} - (|\langle\hat{b}\rangle|^2 + 1)\langle\hat{b}^{\dagger}_{R,k}\hat{b}_{R,k}\rangle(n_{\mathrm{ph},k} + 1)\}, \quad (7)$$

$$\partial\langle\hat{c}^{\dagger}_{R,q}\hat{c}_{R,q}\rangle/\partial t = -\gamma_{\mathrm{IX}}\langle\hat{c}^{\dagger}_{R,q}\hat{c}_{R,q}\rangle + W\sum_{k}\{|\langle\hat{c}\rangle|^2(\langle\hat{c}^{\dagger}_{R,k}\hat{c}_{R,k}\rangle + 1)n_{\mathrm{ph},k} - (|\langle\hat{c}\rangle|^2 + 1)\langle\hat{c}^{\dagger}_{R,k}\hat{c}_{R,k}\rangle(n_{\mathrm{ph},k} + 1)\}, \quad (8)$$

where $\langle\ldots\rangle = \mathrm{Tr}\{\ldots\rho\}$ denotes averaging using the density matrix ρ. Here, we applied the rotating wave approximation $\langle\hat{a}_i\rangle \rightarrow \langle\hat{a}_i\rangle e^{-i\omega_C t}$, and introduced the photonic $\delta_\Omega = \omega_C - \omega_{\mathrm{DX}}$ and excitonic $\delta_J = \omega_{\mathrm{IX}} - \omega_{\mathrm{DX}}$ detunings. The pumping amplitude reads as $\tilde{P}(t) = P_0(t)e^{-i\Delta t}/\hbar$, where $\Delta = \omega_P - \omega_C$ denotes detuning of the coherent optical pumping. The damping rates of the modes are defined by parameters $\gamma_i = 2\pi/\tau_i$, $i = C$, DX, IX. Typical lifetimes of the modes are $\tau_C \approx 3$ ps, $\tau_{\mathrm{DX}} \approx 1$ ns, and $\tau_{\mathrm{IX}} \approx 100$ ns. The reservoir dynamics is governed by a scattering rate $W = \delta_{\Delta E} D^2_{\mathrm{DX}}$, which is proportional to a square of exciton-phonon interaction constant, and $\delta_{\Delta E}$ is a constant accounting for the energy conservation, which is taken to be inverse broadening of exciton states divided by the square of the Plank constant. For simplicity, we consider $D_{\mathrm{DX}} = D_{\mathrm{IX}}$, assume $N = 4 \times 10^5$ reservoir states, and use total scattering rate $W = 2$ ps^{-1} [17]. $n_{\mathrm{ph},k}$ is the Bose distribution of phonons.

Additionally, we derived dynamic equations for occupation numbers for the modes going to higher order of mean-field theory and verified validity of the system [Eqs. (4)–(8)] for chosen pumping conditions. The former model represents the general description of a dipolariton system and allows for accounting of various decoherent processes including pure and phonon-assisted dephasing, which lead to faster decay of oscillations between modes (see the Supplemental Material [32], section B). The effects of nonlinearities introduced by exciton-exciton interactions are discussed in section C of the Supplemental Material [32].

Results and discussion.—We calculate numerically the dynamics of the system with coupled quasiparticles subjected to a picosecond pulsed optical pumping. The presence of mixing terms between different modes implies the oscillating behavior similar to Rabi flopping in the classical model of a two-level system subjected to a time-varying field. It is important to note that our system has several characteristic frequencies. They are governed by the exciton-photon coupling strength Ω and detuning δ_Ω, and the IX-DX coupling strengths J and detuning δ_J. Additionally, the pumping frequency ω_P governs the efficiency of the pump. Varying these characteristic frequencies, one can control the frequency, magnitude, and damping rate of indirect exciton density oscillations.

While the coupling constants Ω and J are dependent on the geometry of the structure and can hardly be tuned for a given sample, the detunings between modes δ_J and δ_Ω are strongly sensitive to the applied electric field F and the incidence angle of the cavity pump, respectively [21]. Tuning these parameters, one can bring the oscillating dipole system to different regimes. If the cavity mode is far detuned from IX-DX anticrossing, the light-exciton coupling is weak, which will be referred to as the regime I. If the detuning δ_Ω is small, the strong intermixing of IX, DX, and C modes takes place, which corresponds to the regime II.

First, we assume low temperature of the system, when phonon processes are suppressed. The behavior of the system in the regime I is shown in Fig. 2(a) for the detuning $\delta_\Omega = -10$ meV. We observe antiphase oscillations of IX and DX densities with decaying amplitudes. The inset in Fig. 2(a) shows a zoom of long-standing phase-locked oscillations which last for several tens of picoseconds. For the electric field corresponding to the resonance between IX and DX modes, F_0, the frequency of oscillations is given by $\nu \approx J/2\pi = 1.45$ THz. The electric field at resonance is equal to $F_0 = \delta_{I-D}/eL$, where $\delta_{I-D} = E^{(0)}_{\mathrm{IX}} - E^{(0)}_{\mathrm{DX}}$ is an exciton detuning at zero applied field, and L is a separation between QWs centers. Considering $\mathrm{In_{0.1}Ga_{0.9}As/GaAs/In_{0.08}Ga_{0.92}As}$ (10 nm/4 nm/10 nm)

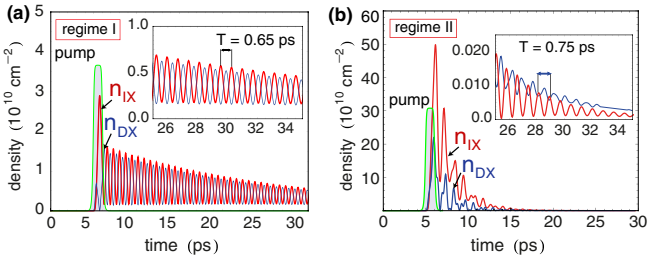

FIG. 2 (color online). Dynamics of the dipolariton system subjected to pulsed optical pumping which shows the oscillations of indirect exciton ($n_{\mathrm{IX}} = |\langle\hat{c}\rangle|^2$) and direct exciton ($n_{\mathrm{DX}} = |\langle\hat{b}\rangle|^2$) density. The coupling constants are equal to $\hbar J = \hbar\Omega = 6$ meV. (a) Oscillations of the density in regime I, where the cavity mode is detuned from direct exciton resonance by $\delta_\Omega = -10$ meV. Pumping frequency is chosen as $\hbar\Delta = 11.5$ meV and electric field $F = 0.95F_0$, where F_0 is the field corresponding to IX-DX resonance. The green area schematically represents the optical pulse with a duration $\Delta\tau = 1$ ps (pump, scaled intensity). The inset shows the long-term term oscillations of $n_{\mathrm{IX}}(t)$ and $n_{\mathrm{DX}}(t)$ density which are in antiphase. The period of oscillations is equal to $T = 0.65$ ps. (b) Oscillations corresponding to regime II, where detuning is equal to $\delta_\Omega = 3$ meV. For the same electrical field and pump intensity ($\hbar\Delta = 0$), the magnitude of the signal is higher comparing to regime I. Inset shows highly damped long-term oscillations in the second regime.

structure studied in Ref. [28], where $\delta_{I-D} = 18$ meV and $L = 14$ nm, it can be calculated as $F_0 \approx 12.8$ kV/cm.

The time dependence of indirect exciton density oscillations $n_{\mathrm{IX}}(t)$, calculated numerically from the Eqs. (4)–(6), can be fitted with the analytical function $n_{\mathrm{IX}}(t) = n^0_{\mathrm{IX}}\cos^2(\omega t/2)e^{-t/\tau}$, where $\omega = 2\pi\nu \approx \sqrt{J^2 + \delta_J^2(F)}$ is the frequency of oscillations and n^0_{IX} denotes the magnitude of oscillations which decreases in time with the damping rate τ^{-1}. Tuning the electric field, the frequency of generated oscillations changes in the range of several THz due to its dependence on IX-DX detuning [Fig. 3(a)], given as $\delta_J(F) = \delta_{I-D}(1 - F/F_0)$ [33]. Other important parameters of the system, such as the amplitude of oscillations and dimensionless oscillation quality factor ξ defined as a ratio of magnitude to the decrement of oscillations, can be tuned by a variation of pumping conditions, as well as by the applied electric field (see the Supplemental Material [32]).

Rising the temperature of the system, the phonon scattering and subsequent population of the reservoir states lead to the increase of characteristic decay rate of the oscillations [Fig. 3(b)]. However, the beats of excitons density are still observable for comparably high frequency and can be exploited in the pulsed regime.

Reducing the detuning between exciton and photon modes δ_Ω, one can bring the system into the regime II. In this regime, the IX density oscillations are observed as well, while their quality factor is different. Strong interactions of the cavity mode with the IX-DX resonance result in a higher magnitude of n_{IX} oscillations than in the regime I [Fig. 2(b)]. The damping rate of these oscillations is also larger. Clearly, the regime of strong coupling between all modes is advantageous for the pulsed pumping regime and it allows for high power generation. On the other hand, the regime I is preferential for the long-standing signal generation providing a higher quality factor ξ, while a lower amplitude of the emission.

We have shown that due to the coupling between modes IX and DX, densities oscillate with a THz frequency. This infers that a dipolariton is an oscillating dipole, with a

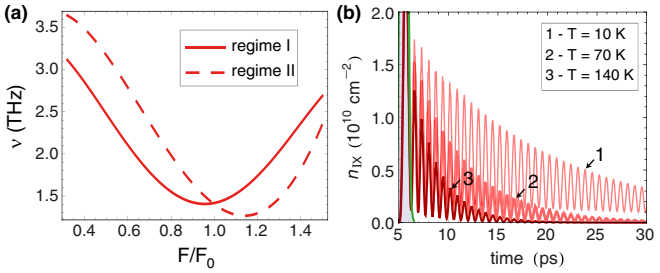

FIG. 3 (color online). (a) Frequency of indirect exciton density oscillations as a function of a dimensionless electric field calculated for oscillations in regime I (solid line) and regime II (dashed line). (b) Indirect exciton density oscillations calculated for different temperatures of the phonon bath. Parameters correspond to regime I.

dipole moment in z direction d_z changing periodically from value $d_z = d_0$ of IX to $d_z = 0$ corresponding to DX. One can define the total dipole moment of the system as $D_z = N_{\mathrm{IX}}d_z$, where $N_{\mathrm{IX}} = n_{\mathrm{IX}}A$ is the number of indirect excitons within the area A illuminated by the pumping light. Since we have shown before that after the initial transient regime the density of indirect excitons $n_{\mathrm{IX}}(t)$ is a decaying harmonic function of time, the total dipole moment of the system can be found as $D_z(t) = d_0 n_{\mathrm{IX}} A\cos^2(\omega t/2)e^{-t/\tau}$. Here, n_{IX} is the maximum density of indirect excitons.

The total intensity of the far field radiation emitted by a classical Hertz dipole can be found as $I = \ddot{D}_z^2/6\pi\epsilon_0 c^3$ [34], where D_z is the total dipole moment of the dipolariton array, ϵ_0 is vacuum permittivity, and c is the speed of light. For the particular case of an array of harmonic dipole oscillations, the intensity is $I = N_{\mathrm{IX}}^2 d_0^2 \omega^4/48\pi\epsilon_0 c^3$, where $d_0 = eL$ is a dipole moment of indirect exciton. Here, for simplicity, we did not consider the damping part $e^{-t/\tau}$ of oscillations. It will result in damping of the total power of emission, which is why to achieve stable cw radiation, one, therefore, needs to use a sequence of pump pulses. Similarly to the conventional case of an elementary dipole emitter, the polar pattern is given by $I_\theta \sim \sin^2\theta$, where θ is an angle between the direction of the radiation and the growth axis of the structure (see the Supplemental Material [32]).

It is important to note that the total emitted intensity is proportional to the square of the density of indirect excitons and is dependent on the pump intensity in a nonlinear way. This is a manifestation of the *superradiance* [35–37] effect: due to the interference of coherent in-phase oscillations of elementary dipoles, the output power is enhanced. This effect is sensitive to the quality factor of the cavity: the longer Rabi oscillations persist, the stronger the amplification effect is. Superradiance is a specific feature of the dipolariton THz emitter, which makes it more efficient than any existing laser-to-THz converter.

For $\hbar J = 6$ meV and the typical distance between QWs of $L = 14$ nm, the power of THz emission of an elementary dipole formed by a dipolariton is $I_0 = 1.5 \times 10^{-18}$ W $= 1.5$ aW. The total power emitted is given by this quantity multiplied by the square number of elementary dipoles N_{IX}. For the typical concentration of indirect excitons achievable experimentally for $n_{\mathrm{IX}} = 10^{10}$ cm^{-2} and a 68 μm diameter of the pumping spot, one obtains $I_{\mathrm{tot}} \approx 2$ μW. By embedding a stack of double quantum wells $n_{\mathrm{DQW}} = 4$ in each microcavity and using several sets of cavities on one chip, one can obtain the output power similar to one of the quantum cascade lasers. Furthermore, to improve the efficiency of THz radiation, the system can be placed in an external cavity tuned to the THz frequency [6,38], with efficiency of emission being increased by the Purcell factor of the external cavity (see the Supplemental Material [32], Fig. S5, for a sketch of setup).

Conclusions.—We have shown that the system of dipolaritons can provide an efficient tunable source of THz radiation. In this system, due to the direct-indirect exciton coupling, the optically excited dipolariton system exhibits density oscillations with a subpicosecond period. The dipole oscillations lead to the superradiant emission of radiation in the THz frequency range. The spectral properties as well as the power output of this system are expected to be strongly improved with respect to the existing laser induced THz emitters. Additionally, we propose a way to enhance the radiation efficiency using a supplementary THz cavity in the weak coupling regime.

We thank Jeremy J. Baumberg and Sven Höfling for useful discussions on the subject. This work has been supported by FP7 IRSES Projects POLATER and POLAPHEN. O. K. acknowledges support from the Eimskip Fund. A. K. acknowledges support from the Russian Ministry of Science and Education. I. A. S. acknowledges the support of Tier 1 Project "Novel Polaritonic Devices."

[1] P. H. Siegel, IEEE Trans. Microwave Theory Tech. **50**, 910 (2002).
[2] G. P. Gallerano and S. Biedron, in *Proceedings of the 2004 FEL Conference, Trieste, Italy, 2004* (Comitato Conferenze Elettra, Trieste, 2004), p. 216.
[3] H. Eisele, IEEE Trans. Microwave Theory Tech. **48**, 626 (2000).
[4] J. Faist, F. Capasso, D. L. Sivco, C. Sirtori, A. L. Hutchinson, and A. Y. Cho, Science **264**, 553 (1994).
[5] R. Köhler, A. Tredicucci, F. Beltram, H. E. Beere, E. H. Linfield, A. G. Davies, D. A. Ritchie, R. C. Iotti, and F. Rossi, Nature (London) **417**, 156 (2002).
[6] M. Geiser, F. Castellano, G. Scalari, M. Beck, L. Nevou, and J. Faist, Phys. Rev. Lett. **108**, 106402 (2012).
[7] D. H. Auston, K. P. Cheung, J. A. Valdmanis, and D. A. Kleinman, Phys. Rev. Lett. **53**, 1555 (1984).
[8] C. Fattinger and D. Grischkowsky, Appl. Phys. Lett. **54**, 490 (1989).
[9] J. Shan and T. F. Heinz, Top. Appl. Phys. **92**, 59 (2004).
[10] M. B. Johnston, D. M. Whittaker, A. Corchia, A. G. Davies, and E. H. Linfield, Phys. Rev. B **65**, 165301 (2002).
[11] O. V. Kibis, M. R. da Costa, and M. E. Portnoi, Nano Lett. **7**, 3414 (2007).
[12] K. G. Batrakov, O. V. Kibis, P. P. Kuzhir, M. R. da Costa, and M. E. Portnoi, J. Nanophoton. **4**, 041665 (2010).
[13] A. M. Alexeev and M. E. Portnoi, Phys. Rev. B **85**, 245419 (2012).
[14] A. V. Kavokin, J. J. Baumberg, G. Malpuech, and F. P. Laussy, *Microcavities* (Oxford University Press, Oxford, 2007).
[15] T. C. H. Liew, I. A. Shelykh, and G. Malpuech, Physica (Amsterdam) **43E**, 1543 (2011).
[16] K. V. Kavokin, M. A. Kaliteevski, R. A. Abram, A. V. Kavokin, S. Sharkova, and I. A. Shelykh, Appl. Phys. Lett. **97**, 201111 (2010).
[17] I. G. Savenko, I. A. Shelykh, and M. A. Kaliteevski, Phys. Rev. Lett. **107**, 027401 (2011).
[18] E. del Valle and A. V. Kavokin, Phys. Rev. B **83**, 193303 (2011).
[19] A. V. Kavokin, I. A. Shelykh, T. Taylor, and M. M. Glazov, Phys. Rev. Lett. **108**, 197401 (2012).
[20] T. C. H. Liew, M. M. Glazov, K. V. Kavokin, I. A. Shelykh, M. A. Kaliteevski, and A. V. Kavokin, Phys. Rev. Lett. **110**, 047402 (2013).
[21] P. Cristofolini, G. Christmann, S. I. Tsintzos, G. Deligeorgis, G. Konstantinidis, Z. Hatzopoulos, P. G. Savvidis, and J. J. Baumberg, Science **336**, 704 (2012).
[22] Yu. E. Lozovik and V. I. Yudson, Sov. Phys. JETP **44**, 389 (1976).
[23] L. V. Butov, A. L. Ivanov, A. Imamoglu, P. B. Littlewood, A. A. Shashkin, V. T. Dolgopolov, K. L. Campman, and A. C. Gossard, Phys. Rev. Lett. **86**, 5608 (2001).
[24] D. Snoke, Science **298**, 1368 (2002).
[25] A. A. High, J. R. Leonard, A. T. Hammack, M. M. Fogler, L. V. Butov, A. V. Kavokin, K. L. Campman, and A. C. Gossard, Nature (London) **483**, 584 (2012).
[26] O. Kyriienko, E. B. Magnusson, and I. A. Shelykh, Phys. Rev. B **86**, 115324 (2012).
[27] G. Christmann, C. Coulson, J. J. Baumberg, N. T. Pelekanos, Z. Hatzopoulos, S. I. Tsintzos, and P. G. Savvidis, Phys. Rev. B **82**, 113308 (2010).
[28] G. Christmann, A. Askitopoulos, G. Deligeorgis, Z. Hatzopoulos, S. I. Tsintzos, P. G. Savvidis, and J. J. Baumberg, Appl. Phys. Lett. **98**, 081111 (2011).
[29] K. Sivalertporn, L. Mouchliadis, A. L. Ivanov, R. Philp, and E. A. Muljarov, Phys. Rev. B **85**, 045207 (2012).
[30] M. Bayer, V. B. Timofeev, F. Faller, T. Gutbrod, and A. Forchel, Phys. Rev. B **54**, 8799 (1996).
[31] O. Kyriienko and I. A. Shelykh, Phys. Rev. B **84**, 125313 (2011).
[32] See Supplemental Material at http://link.aps.org/supplemental/10.1103/PhysRevLett.111.176401 for details of derivation and additional analysis.
[33] L. V. Butov, J. Phys. Condens. Matter **16**, R1577 (2004).
[34] L. D. Landau and E. M. Lifshitz, *The Classical Theory of Fields* (Butterworth-Heinemann, Oxford, 1980).
[35] R. H. Dicke, Phys. Rev. **93**, 99 (1954).
[36] J. G. Bohnet, Z. Chen, J. M. Weiner, D. Meiser, M. J. Holland, and J. K. Thompson, Nature (London) **484**, 78 (2012).
[37] V. I. Yukalov and E. P. Yukalova, Phys. Rev. B **81**, 075308 (2010).
[38] C. Walther, G. Scalari, M. I. Amanti, M. Beck, and J. Faist, Science **327**, 1495 (2010).